Journal of
Synchrotron
Radiation

ISSN 0909-0495

Received 26 December 2008
Accepted 14 March 2009

Universal function for the brilliance of undulator radiation considering the energy spread effect

Takashi Tanaka* and Hideo Kitamura

RIKEN SPring-8 Center, Koto 1-1-1, Sayo, Hyogo 679-5148, Japan. E-mail: ztanaka@spring8.or.jp

Angular and spatial profiles of undulator radiation have been investigated to derive a universal function that evaluates the brilliance of undulator radiation and takes into account the effects of electron beam emittance and energy spread. It has been found that the effects of energy spread on the angular divergence and source size can be expressed by simple analytic expressions, and a universal brilliance function has been derived by convolution with the electron beam distribution functions. Comparisons with numerical results have been carried out to show the validity and applicability of the universal function.

Keywords: undulator radiation; universal function; brilliance; emittance; energy spread.

1. Introduction

Brilliance, which is usually defined by the photon flux density in the phase space spanned by position and angle, is a common figure of merit to specify the performance of a synchrotron radiation (SR) source. It specifies the number of photons in the phase space, and thus is strongly associated with the throughput of a SR beamline.

Strictly speaking, brilliance should be calculated by the method based on the theory of Wigner (Kim, 1986) as a function in four-dimensional phase space (x, y, x', y'). The brilliance distribution should then be convoluted with the electron beam distribution function in order to take into account the effects of the emittance and energy spread. If the experimental users of SR need to know the exact profile of brilliance in the four-dimensional phase space, the above method should be adopted. In practice, however, the brilliance is usually evaluated only on-axis, *i.e.* at the observation point $x = y = x' = y' = 0$ (on-axis brilliance, hereinafter simply called brilliance), just to represent the performance of a SR source.

It is well known that the brilliance is quite sensitive to the quality of the electron beam: lower beam quality results in significant degradation of brilliance, especially in the case of undulator radiation (UR). It is therefore important to evaluate the effects of the electron beam quality, such as the emittance and energy spread. This actually requires a complicated numerical analysis using a large number of parameters to specify the SR source and accelerator performance, which is usually bulky for those who are not familiar with numerical methods or accelerator physics. This is the reason why a number of computer codes have been developed (Walker & Diviacco, 1991; Chubar & Elleaume, 1998; Tanaka & Kitamura, 2001) to compute the brilliance of various kinds of SR sources. Although the brilliance can be precisely evaluated by means of these codes, it takes some time to obtain the computation results. In addition, these codes do not help the SR users understand the mechanism of how the electron beam quality contributes to the brilliance degradation.

Instead of the numerical analysis described above, a simple method can be applied, in which the brilliance is obtained by dividing the total photon flux by the effective optical emittance obtained by convolution between the natural optical emittance determined by the diffraction limit, and the electron beam emittance. This method enables the brilliance calculation only with computation of the Bessel functions of the first kind and several elementary functions, and thus has usually been used to evaluate the performance of a SR facility. It should be noted, however, that the effect of the energy spread is assumed to be negligible in the above method. This assumption is valid if the effect of the beam emittance is much larger than that of the energy spread, which is the case for a typical third-generation SR facility with a beam emittance of 10^{-8} m rad and an energy spread of 10^{-3}.

Although the above conventional method can be applied in many cases, care should be taken if the undulator periodic number is large and/or the harmonic number of UR is high. Furthermore, the effect of the energy spread can be comparable with or larger than that of the finite emittance in SR facilities that accommodate accelerators to generate a high-quality electron beam, which will soon be available thanks to the evolution of accelerator theories and technologies, such as ultra-low-emittance storage rings or energy recovery linacs. In a worst case, the conventional method can overestimate brilliance in such SR facilities by up to two orders of magnitude. Thus the conventional formula should be improved to take into account the effects of the energy spread as well as the emittance for more precise evaluation of brilliance.

In this paper, a new analytic expression is derived as a universal function to evaluate the brilliance of UR. Then the universal function is compared with the conventional method and numerical analysis in order to investigate its validity and applicability.

2. Analytical method

2.1. Basic formulae on UR

Let us first start with the complex amplitude of radiation emitted by a single electron, which is given by the temporal Fourier transform of the electric field (Chubar & Elleaume, 1998; Tanaka & Kitamura, 2001),

$$\mathbf{E}_\omega = \frac{e}{4\pi\varepsilon_0 c} i\omega \int_{-\infty}^{\infty} \frac{1}{R(t')}\left\{\boldsymbol{\beta}(t') - \left[1+\frac{ic}{\omega R(t')}\right]\mathbf{n}(t')\right\} \times \exp[i\omega t(t')]\,\mathrm{d}t' \equiv \frac{e}{4\pi\varepsilon_0 c}\mathbf{F}_\omega, \tag{1}$$

with

$$\mathbf{R}(t') = \mathbf{r} - \mathbf{r}'(t'),$$

$$\mathbf{n}(t') = \mathbf{R}(t')/R,$$

$$t(t') = t' + R(t')/c,$$

where ε_0 is the dielectric constant of vacuum, c is the speed of light, e is the electron charge, ω is the photon energy, $\mathbf{r} = (X, Y, Z)$ is the position of observation, and $\mathbf{r}(t') = (x, y, z)$ and $\boldsymbol{\beta}(t') = (\beta_x, \beta_y, \beta_z)$ specify the position and velocity of the electron at the retarded time t'. Using the complex amplitude $\mathbf{F}_\omega$, the spatial flux density at $\mathbf{r}$ is calculated as

$$\frac{\mathrm{d}^2 N}{\mathrm{d}S\,\mathrm{d}\omega/\omega} = \frac{\alpha}{4\pi^2}|\mathbf{F}_\omega|^2, \tag{2}$$

where α is the fine-structure constant.

Under the far-field approximation, *i.e.* $|\mathbf{r}| \gg |\mathbf{r}'|$ and $\mathbf{R} \simeq \mathbf{r}$ = a constant, equation (1) is simplified to

$$\mathbf{F}_\omega = \frac{i\omega}{cR}\int_{-\infty}^{\infty}[\boldsymbol{\beta}(z) - \mathbf{n}]\exp[i\omega t(z)]\,\mathrm{d}z, \tag{3}$$

with

$$\mathbf{n} = \left(\theta_x, \theta_y, 1 - \theta_x^2/2 - \theta_y^2/2\right) \equiv \left(\theta_x, \theta_y, 1 - \theta^2/2\right),$$

$$t(z) = \frac{1}{2c}\left\{\frac{z}{\gamma^2} + \int_0^z \left[(\beta_x - \theta_x)^2 + \left(\beta_y - \theta_y\right)^2\right]\mathrm{d}z + \theta^2 Z\right\},$$

where γ is the Lorentz factor of the electron and we have introduced the observation angles $\theta_{x,y}$ and changed the integration variable from t' to z/c.

Now let us consider the complex amplitude of radiation for the planar undulator with the number of periods N. Assuming that the magnetic field is ideal, *i.e.* purely sinusoidal in the vertical plane, the relative velocity is given by

$$\beta_x(z) = \begin{cases} (K/\gamma)\cos(k_u z) & |z| \le N\lambda_\mathrm{u}/2, \\ 0 & |z| > N\lambda_\mathrm{u}/2, \end{cases}$$

$$\beta_y(z) = 0,$$

where λ_u is the periodic length and K is the deflection parameter of the undulator.

Substituting the above formulae into equation (3) and expanding into a Fourier series, we have

$$\mathbf{F}_\omega = N\sum_n \mathbf{f}_n(\gamma, \theta_x, \theta_y)\,\mathrm{sinc}\left[n\pi N\frac{\omega - \omega_n(\gamma,\theta)}{\omega_n(\gamma,\theta)}\right]\exp\left(i\omega\frac{\theta^2 Z}{2c}\right), \tag{4}$$

with

$$\mathrm{sinc}\,(x) = \frac{\sin x}{x},$$

$$\omega_n(\gamma,\theta) = n\frac{4\pi c\gamma^2/\lambda_\mathrm{u}}{1 + K^2/2 + \gamma^2\theta^2},$$

$$\mathbf{f}_n\left(\gamma, \theta_x, \theta_y\right) = \frac{i\omega_n(\gamma,\theta)}{cR}\int_0^{\lambda_\mathrm{u}}[\boldsymbol{\beta}(z) - \mathbf{n}]\exp\left(\frac{i\omega_n(\theta,\gamma)}{2c} \times \left\{\frac{z}{\gamma^2} + \int_0^z\left[(\beta_x - \theta_x)^2 + \theta_y^2\right]\mathrm{d}z\right\}\right)\mathrm{d}z,$$

where ω_n is the peak energy of the nth harmonic radiation.

Equation (4) gives the complex amplitude observed at a position far from the source point and thus gives the angular distribution. The spatial distribution at the same position is obtained by the spatial Fourier transform of $\mathbf{F}_\omega$. In order to evaluate the brilliance, however, we need to know the distribution functions at the source point, *i.e.* the beam waist position, which can be found by propagating the radiation back to the source point. From the theory of wave optics, it is found that such backward propagation is given by the mathematical operation (see, for example, Born & Wolf, 1984)

$$\mathbf{F}_{\omega,o} = \mathbf{F}_\omega\exp\left(-i\,\frac{\omega\theta^2 Z}{2c}\right),$$

where we have assumed that the distance from the source point to the observer equals Z, which is valid because the source point of UR exists at the mid-point of the undulator. Substituting equation (4) into the above formula, we have

$$\mathbf{F}_{\omega,o} = N\sum_n \mathbf{f}_n(\gamma, \theta_x, \theta_y)\,\mathrm{sinc}\left[n\pi N\frac{\omega - \omega_n(\gamma,\theta)}{\omega_n(\gamma,\theta)}\right]. \tag{5}$$

The function $\mathbf{F}_{\omega,o}$ gives the angular distribution of the complex amplitude at the source point, while its spatial Fourier transform gives the spatial distribution.

Now let us consider the case when the electron has an energy offset $\Delta\gamma$ compared with a reference energy γ_0. Then the complex amplitude observed at the energy $\omega_n(\gamma_0, 0)$, which is the nth harmonic energy of UR for the reference electron with γ_0, is given by

$$\mathbf{F}_{\omega,o} \simeq N\,\mathbf{f}_n(\gamma_0, \theta_x, \theta_y)\,\mathrm{sinc}(\Theta^2 - \epsilon), \tag{6}$$

with

$$\Theta = \gamma_0\theta\left(\frac{n\pi N}{1+K^2/2}\right)^{1/2}, \quad (7)$$

$$\epsilon = 2\pi nN\Delta\gamma/\gamma_0, \quad (8)$$

where we have assumed that $\Delta\gamma \ll \gamma_0$. Apart from the constant, the function $\mathbf{F}_{\omega o}$ is given by the product of two factors, *i.e.* $\mathbf{f}_n$ and the sinc function. The former function denotes the complex amplitude of the nth harmonic radiation within one undulator period and thus is a slowly varying function of $\theta_{x,y}$, independent of the number of periods N, while the latter function represents the effects of the coherent summation of radiation emitted over the total undulator length, and is strongly associated with N. Under the condition $N \gg 1$, which is satisfied in most SR beamlines with undulators as light sources, the angular profile is thus dominated by the sinc function, and equation (6) can be simplified to

$$\mathbf{F}_{\omega,o} = N\,\mathbf{f}_n(\gamma_0, 0, 0)\,\mathrm{sinc}(\Theta^2 - \epsilon). \quad (9)$$

Note that this simplification gives rise to an error in brilliance evaluation especially for higher harmonics, as discussed later.

Equations (7)–(9) are the basic formulae for studying the effects of electron-beam energy spread on brilliance, which will be discussed in the following sections. Note that these equations are valid for any types of undulators, such as the helical, elliptical and figure-8 undulators, except that $\mathbf{f}_n$ should be recalculated according to the electron trajectory in the concerned undulator, and K^2 should be replaced by $K_x{}^2 + K_y{}^2$, where K_x and K_y are the horizontal and vertical deflection parameters, respectively. In addition, a reservation should be made for even harmonics of planar undulators and for higher harmonics ($n > 1$) of helical undulators, because $\mathbf{f}_n$ vanishes on-axis ($\theta_{x,y} = 0$).

2.2. Angular profile

Substituting equation (9) into (2), we have the angular profile of the flux density at the photon energy $\omega_n(\gamma_0,0)$,

$$\frac{\mathrm{d}^2N}{\mathrm{d}\Omega\,\mathrm{d}\omega/\omega} = \frac{\mathrm{d}^2N_0}{\mathrm{d}\Omega\,\mathrm{d}\omega/\omega}\mathrm{sinc}^2(\Theta^2 - \epsilon),$$

where the function $\mathrm{d}^2N_0/\mathrm{d}\Omega(\mathrm{d}\omega/\omega)$ denotes the flux density on axis ($\Theta = 0$), which is given by the well known expression on UR (see, for example, Kim, 1989),

$$\frac{\mathrm{d}^2N_0}{\mathrm{d}\Omega\,\mathrm{d}\omega/\omega} = \alpha N^2\gamma_0^2K^2\xi^2\left[J_{\frac{n+1}{2}}(K^2\xi/4) - J_{\frac{n-1}{2}}(K^2\xi/4)\right]^2, \quad (10)$$

with

$$\xi = \frac{n}{1+K^2/2},$$

where J_m is the mth-order Bessel function of the first kind.

Let us consider the effects of the energy spread of the electron beam. Assuming the energy distribution function to be a Gaussian function with the standard deviation σ_E, we have

$$\frac{\mathrm{d}^2N_e}{\mathrm{d}\Omega\,\mathrm{d}\omega/\omega} = \frac{\mathrm{d}^2N_0}{\mathrm{d}\Omega\,\mathrm{d}\omega/\omega}P_a(\Theta, \sigma_\epsilon) \quad (11)$$

with

$$P_a(\Theta, \sigma_\epsilon) = \frac{1}{(2\pi)^{1/2}\sigma_\epsilon}\int_{-\infty}^{\infty}\mathrm{sinc}^2(\Theta^2 - \epsilon)\exp\left(-\frac{\epsilon^2}{2\sigma_\epsilon^2}\right)\mathrm{d}\epsilon, \quad (12)$$

where we have introduced the normalized energy spread σ_ϵ defined as

$$\sigma_\epsilon = 2\pi nN\sigma_E. \quad (13)$$

Fig. 1(*a*) shows the graphical plot of P_a for different values of σ_ϵ. It is found that the peak value at $\Theta = 0$ decreases and the peak is broadened as σ_ϵ increases.

Let us approximate the function P_a by the two-dimensional Gaussian function with the standard deviation σ_Θ, *i.e.*

$$P_a(\Theta, \sigma_\epsilon) = P_a(0, \sigma_\epsilon)\exp\left(-\frac{\Theta^2}{2\sigma_\Theta^2}\right).$$

Integrating over Θ, we have

$$\sigma_\Theta = \left[\frac{S_a(\sigma_\epsilon)}{2\pi P_a(0, \sigma_\epsilon)}\right]^{1/2}, \quad (14)$$

with

$$S_a(\sigma_\epsilon) = 2\pi\int\Theta P_a(\Theta, \sigma_\epsilon)\,\mathrm{d}\Theta.$$

Now let us show that S_a is independent of σ_ϵ and is equal to $\pi^2/2$. First let us modify the above equation as follows,

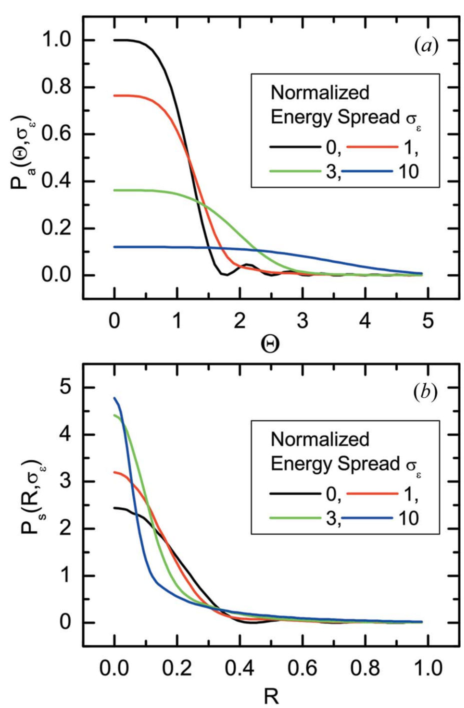

Figure 1
(*a*) Angular profile function P_a and (*b*) spatial profile function P_s for different values of σ_ϵ.

$$
\begin{aligned}
S_a &= \pi \int_0^\infty \mathrm{d}\vartheta \int_{-\infty}^{\infty} \mathrm{d}\epsilon \frac{1}{(2\pi)^{1/2}\sigma_\epsilon} \operatorname{sinc}^2\vartheta \exp\left[-\frac{(\vartheta-\epsilon)^2}{2\sigma_\epsilon^2}\right] \\
&\equiv \pi \int_0^\infty \mathrm{d}\vartheta\, I(\vartheta).
\end{aligned}
$$

Thus, S_a is the area of $I(\vartheta)$ obtained by integrating from 0 to ∞. The function $I(\vartheta)$ is obtained by convoluting $\operatorname{sinc}^2\vartheta$ with the Gaussian function having the total area (obtained by integrating from $-\infty$ to ∞) of unity. From the theory of convolution, it is therefore obvious that the total area of $I(\vartheta)$ is the same as that of $\operatorname{sinc}^2\vartheta$, *i.e.* π. In addition, $I(\vartheta)$ is an even function because both $\operatorname{sinc}^2(\vartheta)$ and the Gaussian function are even functions. Thus we obtain $S_a = \pi^2/2$.

As for $P_a(0,\sigma_\epsilon)$, the integration can be performed analytically to give

$$
\begin{aligned}
P_a(0,\sigma_\epsilon) &= \frac{1}{(2\pi)^{1/2}\sigma_\epsilon} \int_{-\infty}^{\infty} \operatorname{sinc}^2\epsilon \exp\left(-\frac{\epsilon^2}{2\sigma_\epsilon^2}\right) \mathrm{d}\epsilon \\
&= \frac{-1+\exp(-2\sigma_\epsilon^2)+(2\pi)^{1/2}\sigma_\epsilon \operatorname{erf}(2^{1/2}\sigma_\epsilon)}{2\sigma_\epsilon^2}, \qquad (15)
\end{aligned}
$$

with

$$
\operatorname{erf}(x) = \frac{2}{\pi^{1/2}} \int_0^x \exp\left(-t^2\right) \mathrm{d}t
$$

being the Gauss error function.

Now we can calculate the angular divergence $\sigma_{r'}$ of UR with the effects of the energy spread taken into account. Substituting the above results into equation (14) and considering equation (7), we have

$$
\begin{aligned}
\sigma_{r'}(\sigma_\epsilon) &= \frac{1}{\gamma_0}\left(\frac{1+K^2/2}{\pi n N}\right)^{1/2}\left[\frac{S_a}{2\pi P_a(0,\sigma_\epsilon)}\right]^{1/2} \\
&= \left(\frac{\lambda_n}{2L}\right)^{1/2} Q_a(\sigma_\epsilon) = \sigma_{r'0} Q_a(\sigma_\epsilon), \qquad (16)
\end{aligned}
$$

with

$$
\lambda_n = 2\pi c/\omega_n(\gamma_0, 0),
$$

$$
Q_a(x) = \left[\frac{2x^2}{-1+\exp(-2x^2)+(2\pi)^{1/2} x \operatorname{erf}(2^{1/2}x)}\right]^{1/2}, \qquad (17)
$$

where λ_n is the wavelength of the nth harmonic radiation and L is the total length of the undulator. The parameter $\sigma_{r'0}$, which is the angular divergence of UR at $\sigma_\epsilon = 0$, is the well known expression found in textbooks on SR (see, for example, Kim, 1989). Equation (16) indicates that the angular divergence grows according to the energy spread by the factor Q_a.

Fig. 2(*a*) shows a graphical plot of the growth factor $Q_a = \sigma_{r'}(\sigma_\epsilon)/\sigma_{r'0}$ as a function of the normalized energy spread σ_ϵ. Note that Q_a has a minimum value of 1 at $\sigma_\epsilon = 0$, and becomes greater for larger σ_ϵ values. For example, Q_a reaches 2 around $\sigma_\epsilon = 5$, meaning that the angular divergence is doubled owing to the effects of the energy spread.

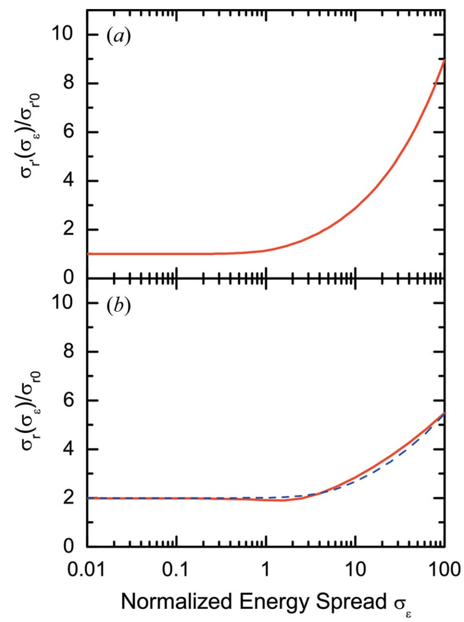

Figure 2
Effects owing to the energy spread of the electron beam on (*a*) the angular divergence and (*b*) the source size. The blue (dashed) line in (*b*) shows the fitting function to approximate the source size growth factor.

2.3. Spatial profile

Next, let us investigate the spatial profile of the flux density at the source point, which is given by taking the square of the spatial Fourier transform of $\mathbf{F}_{\omega,o}$,

$$
\begin{aligned}
\tilde{\mathbf{F}}_{\omega,o}(\boldsymbol{\rho}) &= \int \mathrm{d}\mathbf{k}\, \mathbf{F}_{\omega,o} \exp(i\mathbf{k}\cdot\boldsymbol{\rho}) \\
&= \frac{8\pi^2}{\lambda_n \lambda_u} \mathbf{f}_n(\gamma_0, 0, 0) \int_0^\infty \mathrm{d}\vartheta\, J_0(2\pi\vartheta^{1/2}R) \operatorname{sinc}(\vartheta-\epsilon), \qquad (18)
\end{aligned}
$$

with

$$
R = \frac{\rho}{\lambda_n \gamma_0}\left(\frac{1+K^2/2}{\pi n N}\right)^{1/2} \qquad (19)
$$

being the normalized radial coordinate. Now we have the spatial profile of the flux density at the source point,

$$
\frac{\mathrm{d}^2 N}{\mathrm{d}S\, \mathrm{d}\omega/\omega} \propto P_s(R, \sigma_\epsilon),
$$

with

$$
\begin{aligned}
P_s(R,\sigma_\epsilon) &= \frac{1}{(2\pi)^{1/2}\sigma_\epsilon} \int_{-\infty}^{\infty} \mathrm{d}\epsilon \exp\left(-\frac{\epsilon^2}{2\sigma_\epsilon^2}\right) \\
&\quad \times \left| \int_0^\infty \mathrm{d}\vartheta\, J_0(2\pi\vartheta^{1/2}R) \operatorname{sinc}(\vartheta-\epsilon) \right|^2.
\end{aligned}
$$

If the Gaussian approximation is possible, which has been used to obtain the angular divergence in the previous section, the standard deviation of P_s, *i.e.* the normalized source size Σ_R, can be determined by

$$\Sigma_R(\sigma_\epsilon) = \left[\frac{S_s(\sigma_\epsilon)}{2\pi P_s(0,\sigma_\epsilon)}\right]^{1/2}, \tag{20}$$

with

$$S_s(\sigma_\epsilon) = 2\pi \int_0^\infty R P_s(R,\sigma_\epsilon)\,\mathrm{d}R.$$

Then the source size of UR, which is denoted by σ_r, is given by

$$\sigma_r(\sigma_\epsilon) = \Sigma_R(\sigma_\epsilon)\lambda_n\gamma_0\left(\frac{\pi n N}{1+K^2/2}\right)^{1/2} = 2\pi^{3/2}\Sigma_R(\sigma_\epsilon)\sigma_{r0},$$

with

$$\sigma_{r0} = \frac{(2\lambda_n L)^{1/2}}{4\pi},$$

where σ_{r0} is the well known expression for the source size of UR at $\sigma_\epsilon = 0$ (see, for example, Kim, 1989).

Fig. 1(*b*) shows a graphical plot of P_s for difference values of σ_ϵ. It is found that the peak value at $R = 0$ increases and the peak shrinks as σ_ϵ increases. It should be noted, however, that a long-range tail exists together with the narrow peak around $R = 0$ for larger values of σ_ϵ. Owing to this tail, the Gaussian approximation is not valid and thus equation (20) is not available for larger values of σ_ϵ. Thus we have to modify the above equation in order to utilize the Gaussian approximation as follows.

First, we convolute P_s with the Gaussian function with a standard deviation $\Sigma_{\rm ref}$. If $\Sigma_{\rm ref}$ is large enough, the resultant spatial profile P_s' can be well approximated by the Gaussian function. Then the normalized source size Σ_R', which is determined by P_s', is obtained by applying the same method as in the previous section. Namely,

$$\Sigma_R'(\sigma_\epsilon) = \left[\frac{S_s(\sigma_\epsilon)}{2\pi P_s'(0,\sigma_\epsilon)}\right]^{1/2},$$

with

$$P_s'(0,\sigma_\epsilon) = \frac{1}{\Sigma_{\rm ref}^2}\int \mathrm{d}R\, P_s(R,\sigma_\epsilon) R \exp\left(-2R^2/\Sigma_{\rm ref}^2\right).$$

Because Σ_R' is regarded to be the convolution between $\Sigma_{\rm ref}$ and Σ_R, we have

$$\Sigma_R = \left({\Sigma_R'}^2 - \Sigma_{\rm ref}^2\right)^{1/2}. \tag{21}$$

The value of $\Sigma_{\rm ref}$ should be determined to meet two requirements. Firstly, the convoluted profile P_s' can be well approximated by the Gaussian function. Secondly, Σ_R' is not significantly different from Σ_R. In order to meet the two requirements, we have repeated numerical analysis and found the reasonable condition that $\Sigma_{\rm ref} = 1/\pi^{3/2}$. It is interesting to calculate the source size $\sigma_{\rm ref}$ that corresponds to the normalized source size $\Sigma_{\rm ref}$, namely,

$$\sigma_{\rm ref} = 2\pi^{3/2}\Sigma_{\rm ref}\sigma_{r0} = 2\sigma_{r0}. \tag{22}$$

As shown later, $2\sigma_{r0}$ is found to be the source size of UR at $\sigma_\epsilon = 0$.

Let us define the function $Q_s(\sigma_\epsilon)$ as

$$Q_s(\sigma_\epsilon) = \sigma_r/\sigma_{r0} = 2\pi^{3/2}\Sigma_R(\sigma_\epsilon), \tag{23}$$

which is regarded to be the growth factor of the source size according to the energy spread.

Fig. 2(*b*) shows a graphical plot of $Q_s(\sigma_\epsilon)$ obtained by the numerical analysis described above. It should be noted that $Q_s(0) = 2$, meaning that the source size of UR obtained with the current analysis is larger than the well known expression by a factor of 2. This discrepancy is attributable to the difference in the method of analysis. The well known expression is derived based on the assumption that both the spatial and angular profiles are given by the Gaussian function and thus UR is like a single-mode laser, which is not necessarily valid. Although we also use the Gaussian approximation to determine the angular divergence and source size, the spatial profile has been derived by the spatial Fourier transform of the angular distribution of the complex amplitude, which is more reasonable. The brilliance degradation of UR owing to the non-Gaussian angular profile has also been pointed out by Kim (1986). In addition, the discrepancy may become more pronounced at the detuned photon energy $\omega = \omega_n$ (Coisson, 1988), which is out of scope in this paper.

It is worth noting that the function Q_s can be well fitted using the function Q_a,

$$Q_s(x) = 2\left[Q_a(x/4)\right]^{2/3}. \tag{24}$$

The above fitting function is plotted in Fig. 2(*b*) to be compared with the results obtained by the numerical analysis, where we find a good agreement between the two. Hereinafter, we use the above fitting function to calculate Q_s.

2.4. Evaluation of brilliance

Having determined the angular divergence and source size with the effects of the energy spread taken into account, let us now evaluate the brilliance, which is given by

$$B = \frac{F}{4\pi^2\Sigma_x\Sigma_{x'}\Sigma_y\Sigma_{y'}}, \tag{25}$$

where F is the total flux of radiation emitted over the whole solid angle, and $\Sigma_{x',y'}$ and $\Sigma_{x,y}$ are the angular divergence and source size of the photon beam in the horizontal and vertical directions, respectively. Using the formulae derived in the former sections, we have

$$F = 2\pi\sigma_{r'0}^2 \frac{\mathrm{d}^2 N_0}{\mathrm{d}\Omega\,\mathrm{d}\omega}, \tag{26}$$

$$\Sigma_{x'} = \left(\sigma_{x'}^2 + \sigma_{r'0}^2 Q_a^2\right)^{1/2}, \tag{27}$$

$$\Sigma_x = \left(\sigma_x^2 + \sigma_{r0}^2 Q_s^2\right)^{1/2}, \tag{28}$$

and similar equations for y, where $\sigma_{x'}$ and σ_x are the angular divergence and beam size of the electron beam in the horizontal direction, respectively. Note that we have omitted the argument σ_ϵ of the function Q_a and Q_s for simplicity. Equations (13), (17) and (24)–(28) form a universal function to evaluate the brilliance of undulator radiation, which takes into account the finite emittance and energy spread of the electron beam. This is the conclusion of the discussions so far. Note that the expression on brilliance by the conventional method is obtained by substituting $Q_{a,s}$ = 1 into equations (27) and (28). This means that the conventional formula has been derived with an assumption that the UR is a Gaussian beam and the effects of the energy spread are negligible.

Assuming that the position of the electron beam waist is placed at the source point (mid-point of the undulator) and that the dispersion function is zero, the above equation is simplified to

$$(\Sigma_{x'}\Sigma_x)^2 = \varepsilon_x^2 + 2\varepsilon_x\varepsilon_\lambda Q_s Q_a G(\beta_x/\beta_o) + (\varepsilon_\lambda Q_s Q_a)^2 \equiv E_x^2,$$

with

$$G(x) = \left(x + x^{-1}\right)/2,$$

$$\varepsilon_\lambda = \frac{\lambda_n}{4\pi},$$

$$\beta_o = \frac{L}{2\pi}\frac{Q_s}{Q_a},$$

where β_x is the horizontal betatron value at the mid-point of the undulator, and E_x can be regarded as the emittance of the photon beam with the effects of the electron beam emittance and energy spread (effective optical emittance), while ε_λ is the optical emittance of the Gaussian beam at a wavelength of λ_n.

The factor $G(\beta_x/\beta_o)$ has a minimum value of 1 when $\beta_x = \beta_o$, then E_x is simplified to

$$E_x = \varepsilon_x + \varepsilon_\lambda Q_a Q_s.$$

Thus the effective optical emittance is given by a simple summation of the electron beam emittance (ε_x), and the natural optical emittance (ε_λ) multiplied by the growth factor ($Q_a Q_s$) determined by the energy spread, if the betatron function is optimized.

3. Comparison with numerical results

In order to examine the validity of the expressions derived so far, comparisons with numerical results have been made using *SPECTRA* (Tanaka & Kitamura, 2001), the computer code for numerical analysis on SR characteristics. For this purpose, the code has been revised to implement the function to calculate the spatial profile at the source point with the effects of the energy spread taken into account, which was not implemented in the former version. The brilliance is then evaluated by dividing the angular flux density by the source size, which is obtained from the spatial profile at the source point.

The accelerator and undulator parameters of the third-generation SR facility SPring-8 have been used for the brilliance calculation, and are summarized in Table 1. The length of the standard straight section (S) is around 5 m, in which in-vacuum undulators with L = 4.5 m and λ_u = 32 mm are usually installed for X-ray beamlines. In addition to S, SPring-8 has four long straight sections (LSs) of length 27 m, and a 25 m in-vacuum undulator has been installed in one of them. Because of the large number of periods, the brilliance available with the long undulator in a LS is expected to be sensitive to the energy spread, and thus is well suited for examination of the calculation method.

Table 1
Accelerator and undulator parameters used in the comparisons.

	Straight section	
	S	LS
Accelerator parameters		
Electron energy	8 GeV	8 GeV
Average current	100 mA	100 mA
Natural emittance	3.4×10^{-9} m rad	3.4×10^{-9} m rad
Energy spread	0.001	0.001
Coupling constant	0.002	0.002
β_x	22.28 m	21.7 m
β_y	5.61 m	14.05 m
η_x	0.11 m	0.103 m
Undulator parameters		
λ_u	32 mm	32 mm
K	2	2
$\hbar\omega_1$	6330 eV	6330 eV
L	4.5 m	25 m

The brilliance calculations have been carried out for harmonics between the first and 11th by three different methods, *i.e.* the numerical method with *SPECTRA*, the universal function derived in the former sections, and the conventional formula.

Figs. 3(*a*) and 3(*b*) show the results of calculations in the case of S and LS undulators, respectively. It is found that the conventional formula overestimates the brilliance under all the conditions, and the overestimation depends on the harmonic number and the undulator type, *i.e.* the undulator length. In other words, the brilliance evaluation with the conventional formula is not reliable for large values of the normalized energy spread σ_ϵ. On the other hand, we find a good agreement between the results of the numerical analysis and universal function when the harmonic number is less than, for example, 7. For larger harmonic numbers, the universal function overestimates the brilliance to some extent.

In order to understand the overestimation of brilliance at higher harmonics, let us derive the angular profile of the flux density without approximation. By using equation (6) instead of its simplified form (9), we have

$$\frac{\mathrm{d}^2 N_e}{\mathrm{d}\Omega\,\mathrm{d}\omega/\omega} = \frac{\mathrm{d}^2 N_0}{\mathrm{d}\Omega\,\mathrm{d}\omega/\omega}\rho_n(\theta_x,\theta_y)P_a(\Theta,\sigma_\epsilon), \qquad (29)$$

with

$$\rho_n(\theta_x,\theta_y) \equiv \frac{|f_n(\gamma_0,\theta_x,\theta_y)|^2}{|f_n(\gamma_0,0,0)|^2}.$$

Note that the universal function has been derived under the approximation

$$\rho_n(\theta_x,\theta_y) = \text{a constant} = 1. \qquad (30)$$

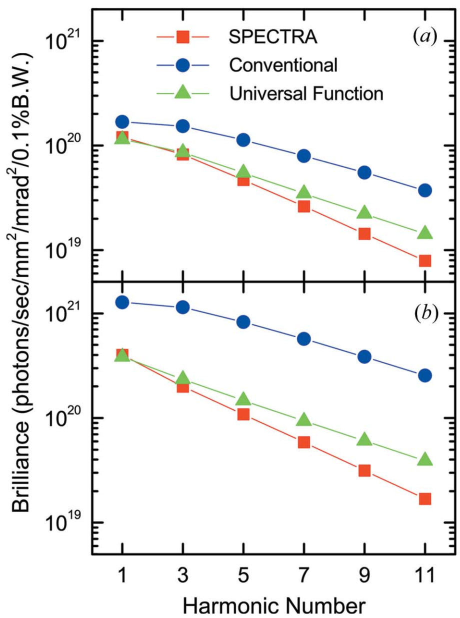

Figure 3
Comparison of brilliance calculated by three different methods. Red (squares): numerical method using *SPECTRA*; blue (circles): conventional formula; green (triangles): universal function. The calculations have been made for harmonic numbers between 1 and 11 in the case of undulators in (*a*) S and (*b*) LS, respectively.

It has been shown in §2.3 that integration of P_a over Θ is constant and thus the total flux F obtained by integrating (29) is found to be independent of the normalized energy spread σ_ϵ as long as the approximation (30) is valid.

In order to examine the applicability of (30), we have calculated the horizontal angular profiles of ρ_n for two different harmonic numbers, 1 and 11, which are plotted in Fig. 4. It is found that ρ_1 is a slowly varying function of θ_x, while ρ_{11} oscillates rapidly. We now find that F decreases more rapidly as σ_ϵ for larger n, which is easily understood by looking to the angular profiles of the two factors P_a and ρ_n shown in Figs. 1(*a*) and 4, respectively. In other words, the approximation (30) becomes less accurate for larger n and N, and the universal function tends to overestimate the brilliance, which coincides with the results shown in Fig. 3.

4. Summary

New analytical expressions have been derived as a universal function to evaluate the brilliance of UR, and have been examined by comparing with numerical analysis. It has been found that the brilliance can be evaluated precisely by the universal function, although care should be taken on its use for higher harmonics.

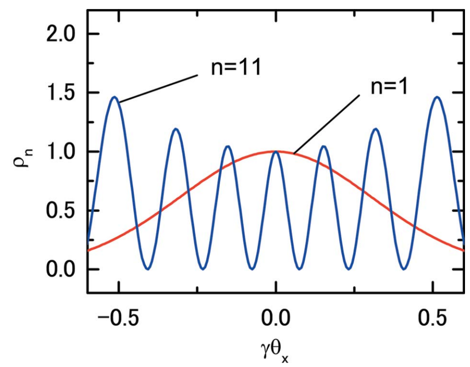

Figure 4
Graphical plot of the function ρ_n for the harmonic numbers 1 and 11.

The universal function contains two special functions, *i.e.* the Bessel function of the first kind and the Gauss error function. The former function is also contained in the conventional formula, while the latter function can be well approximated by a combination of elementary functions (see, for example, Stoer & Bulirsch, 1991). Thus the universal function is easily utilized not only by experts on SR but also by those who are not familiar with the numerical method on SR. Although the brilliance can be evaluated precisely by the numerical codes as already mentioned in the *Introduction*, the universal function derived in this paper is useful for many applications. For example, it can be easily implemented not only in general-purpose computer software for investigating the performance of SR sources but also in specialized codes written for a variety of purposes.

References

Born, M. & Wolf, E. (1984). *Principles of Optics*, 6th ed. New York: Pergamon Press.
Chubar, O. & Elleaume, P. (1998). *Proceedings of the European Particle Accelerator Conference (EPAC-98)*, pp. 1177–1179.
Coisson, R. (1988). *Opt. Eng.* **27**, 250–252.
Kim, K. J. (1986). *Nucl. Instrum. Methods Phys. Res. A*, **246**, 71–76.
Kim, K. J. (1989). *AIP Conf. Proc.* **184**, 565–632.
Stoer, J. & Bulirsch, R. (1991). *Introduction to Numerical Analysis.* New York: Springer-Verlag.
Tanaka, T. & Kitamura, H. (2001). *J. Synchrotron Rad.* **8**, 1221–1228.
Walker, R. P. & Diviacco, B. (1991). *Rev. Sci. Instrum.* **63**, 392–395.